

# First observations of detached equatorial ionospheric plasma depletions using OI 630.0 nm and OI 777.4 nm emissions nightglow imaging

Y. Sahai,<sup>1</sup> J. R. Abalde,<sup>1</sup> P. R. Fagundes,<sup>1</sup> V. G. Pillat,<sup>1</sup> and J. A. Bittencourt<sup>2</sup>

Received 18 November 2005; revised 3 March 2006; accepted 21 April 2006; published 6 June 2006.

[1] Near-simultaneous all-sky (180° field of view) observations of the OI 630.0 nm and OI 777.4 nm nightglow emissions are being carried out on a routine basis at “Laboratório Nacional de Astrofísica (LNA)”, Brazópolis (22.5° S, 45.6° W; dip latitude 17.5° S; altitude 1860 m), Brazil, since September 2002. The all-sky imaging observations of the OI 630.0 nm and OI 777.4 nm emissions, which arise from the dissociative recombination of O<sub>2</sub><sup>+</sup> ions and radiative recombination of O<sup>+</sup> ions (mainly), respectively, are used to monitor the morphology and dynamics of the equatorial F-region at the respective emission heights. In this paper we present and discuss the first observations showing detached equatorial F-region plasma depletions or bubbles. Three cases are presented from observations during the years 2002 and 2003. We suggest a possible mechanism for their generation. **Citation:** Sahai, Y., J. R. Abalde, P. R. Fagundes, V. G. Pillat, and J. A. Bittencourt (2006), First observations of detached equatorial ionospheric plasma depletions using OI 630.0 nm and OI 777.4 nm emissions nightglow imaging, *Geophys. Res. Lett.*, 33, L11104, doi:10.1029/2005GL025262.

## 1. Introduction

[2] Equatorial spread-F (ESF) or plasma irregularities associated with the nighttime equatorial F-region continue to be an active subject of intensive investigations. The pioneering air-borne work by *Weber et al.* [1978] and *Moore and Weber* [1981], showed that wide-angle imaging of the F-region nightglow emissions (e.g., OI 630.0 nm and OI 777.4 nm) could be used to study several features related with large scale ionospheric plasma depletions (range type spread-F), generally referred to as trans-equatorial plasma bubbles. Plasma bubbles or depletions are initially generated in the bottomside of the nighttime equatorial F-region, through a fluid-type gradient instability mechanism such as the gravitational Rayleigh-Taylor instability [*Dungey*, 1956; *Ossakow et al.*, 1979; *Zalesak et al.*, 1982]. As plasma bubbles grow in the equatorial region, they carry low electron density flux tubes to high altitudes and extend poleward in the flux tubes as they rise over the magnetic equator [*Sales et al.*, 1996]. The all-sky images of the OI 630.0 nm and OI 777.4 nm emissions show nearly north-

south magnetic field aligned intensity depletion bands which are the optical signatures of the plasma bubbles at the respective peak emission heights.

[3] The OI 630.0 nm emission results from the dissociative recombination of O<sub>2</sub><sup>+</sup> ions in the F-region, produced by the two-step process (O<sup>+</sup> + O<sub>2</sub> → O + O<sub>2</sub><sup>+</sup>; O<sub>2</sub><sup>+</sup> + e → O + O\*) and the emission peak is located in the bottomside of the F-region. The OI 777.4 nm emission in the F-region results mainly from the radiative recombination of O<sup>+</sup> ions (O<sup>+</sup> + e → O\* + hν) and the emission peak is located at the F-region peak. Therefore, wide-angle images at OI 630.0 nm and OI 777.4 nm emissions exhibit plasma density associated with two different altitudes. Also, as mentioned earlier, the ESF or plasma bubbles are electron density depleted flux tubes, so that the wide-angle images at these two emissions show signatures of plasma depleted regions from the respective emission heights.

[4] In this paper we present and discuss the first observations of detached plasma bubbles using near simultaneous ground-based all-sky images of the OI 630.0 nm and OI 777.4 nm nightglow emissions in the tropical region. Also, we suggest a possible mechanism for detachment of plasma bubbles.

## 2. Observations

[5] An all-sky (180° field of view) multi-spectral (OI 777.4 nm, OI 630.0 nm, OI 557.7 nm, NaD 589.3 nm, N<sub>2</sub><sup>+</sup> 427.8 nm, OH (wide-band), O<sub>2</sub> (0,1) band at 864.5 nm emissions) imaging system belonging to UNIVAP was installed for routine operation at “Laboratório Nacional de Astrofísica (LNA)”, Brazópolis (22.5° S, 45.6° W; dip latitude 17.5° S; altitude 1860 m; hereafter referred as LNA), Brazil, in September 2002. The imaging system uses 3 in diameter interference filters with bandwidths of 2.0 and 1.5 nm for the OI 630.0 nm and OI 777.4 nm emissions, respectively. The charged-coupled device (CCD) used is Photometrics model CH350 (back-illuminated bare CCD, 1024x1024 pixel) with high quantum efficiency of about 80% in the visible region. The front-end lens is a fast (f/4) 180° field of view Mamiya 24-mm telecentric system. The observations were carried out using a filter-wheel with 2 min integration time for observations of both the OI 630.0 nm and OI 777.4 nm emissions. The timings shown with images in Figures 1, 2, and 3, refer to the end time. More details of the all-sky imaging system can be found in *Abalde et al.* [2001].

[6] The observed images of different emissions are stored on a PC at the observational site, and, thereafter, processed and analyzed using the programs package developed at

<sup>1</sup>Universidade do Vale do Paraíba (UNIVAP), São José dos Campos, São Paulo, Brazil.

<sup>2</sup>Instituto Nacional de Pesquisas Espaciais (INPE), São José dos Campos, São Paulo, Brazil.

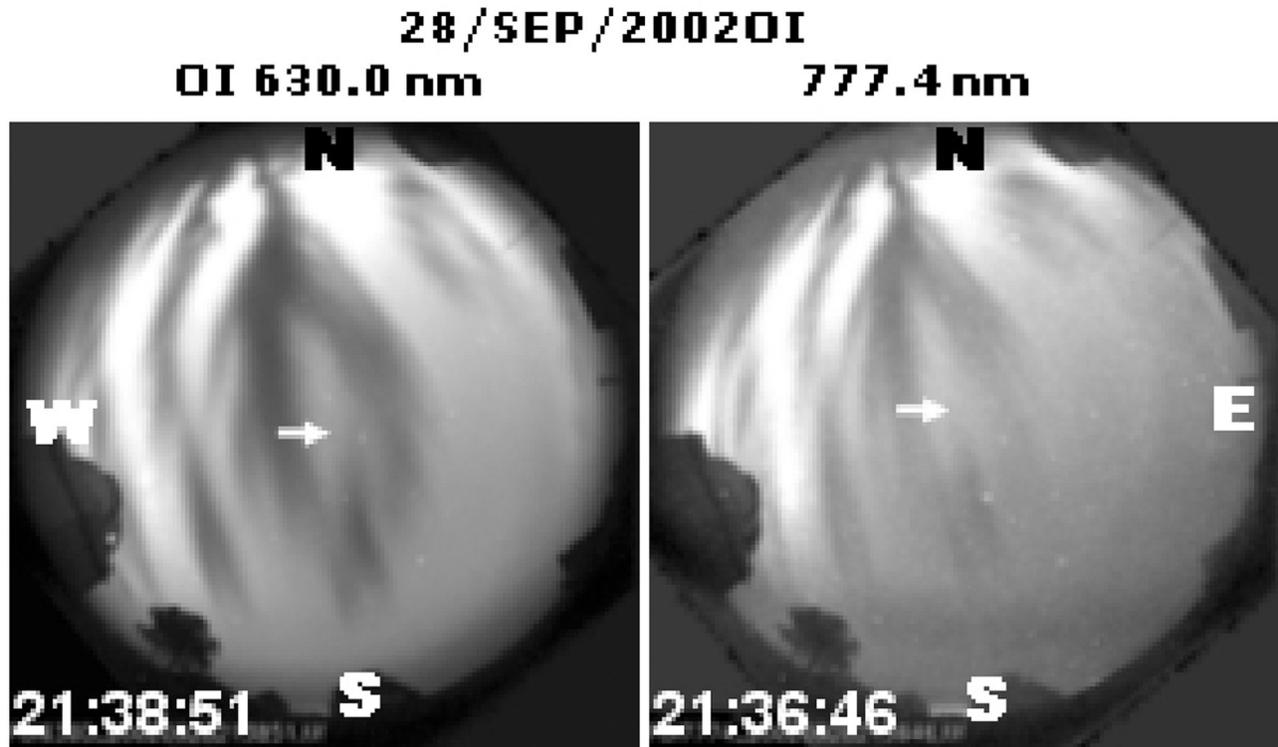


**Figure 1.** Near-simultaneous all-sky images observed at OI 630.0 nm and OI 777.4 nm emissions on 28 September 2002 at 21:38:51 and 21:36:46 LT, respectively. A detached plasma bubble is seen south of the arrow in both the emissions.

UNIVAP, known as “UNIVAP All-sky Data Analysis (UASDA)”.

### 3. Results and Discussion

[7] Figure 1 shows near-simultaneous all-sky imaging observations of the OI 630.0 nm emission (21:38:51 LT) and OI 777.4 nm emission (21:36:46 LT) observed on the night of 28 September 2002 at LNA. Both the emissions show copious presence of large-scale plasma depletions (dark portions). The plasma depleted structures are aligned along the geomagnetic field lines (about  $20^\circ$  declination toward west). It is observed that plasma depleted structures in the OI 777.4 nm emission image show sharp ray-like patterns, whereas the depleted structures in the OI 630.0 nm emission image are diffused or blurred. This difference in the images at these two emission lines has been discussed in detail by *Abalde et al.* [2001] and they are related to the different lifetimes of the corresponding emission excited electronic states. The plasma depleted structures in the middle of the two images (OI 630.0 nm and OI 777.4 nm) clearly show a detached bubble south of the arrow mark. Also, Figure 1 shows multiple bifurcations of the depleted plasma structure [*Aggson et al.*, 1996] in the middle of both the images (north of the arrow mark). It should be pointed out that in the present observation, the principal bifurcation [*Mendillo and Tyler*, 1983; *Huang and Kelley*, 1996; *Aggson et al.*, 1996] took place earlier (not shown) in time and approximately at an apex altitude between 650–700 km. The observed apex height is comparable to 740 km reported

by *Mendillo and Tyler* [1983]. Figure 2 shows a sequence of near-simultaneous linearized images of both the emissions shown in Figure 1. The images were linearized (600 x 600 km area) using the technique described by *Garcia et al.* [1997] and *Pimenta et al.* [2003a], and assuming peak emission heights for the OI 630.0 nm and OI 777.4 nm emissions as 280 and 330 km, respectively. The arrows in Figure 2 show the evolution of plasma bubble with time and eventual detachment in both the emissions from the bifurcated structure.

[8] Figure 3 shows two more sequence of images of the OI 630.0 nm emission observed on the nights of 07 January 2003 and 16 October 2003, with arrows again showing the evolution of plasma bubbles and eventual detachments. Due to low emission intensities, the OI 777.4 nm images are not presented here. The nights of 28–29 September 2002 and 7–8 January 2003 are geo-magnetically quiet. The night of 16–17 October 2003 is in the recovery phase of a very moderate geo-magnetic disturbance with the AE geomagnetic index less than 500 nT around the time of the observed detachment of plasma bubble. This rules out the possibility of penetration/disturbance dynamo electric fields playing a role in the detachment process. However, more case studies will be important to assess the influence of geomagnetic disturbances.

[9] The present results show the first observations of detached plasma bubbles. It should be pointed out that in all the three cases reported, the west arm of the bifurcated plasma bubble got detached. From many previous studies it is well understood that the western wall is (typically) the

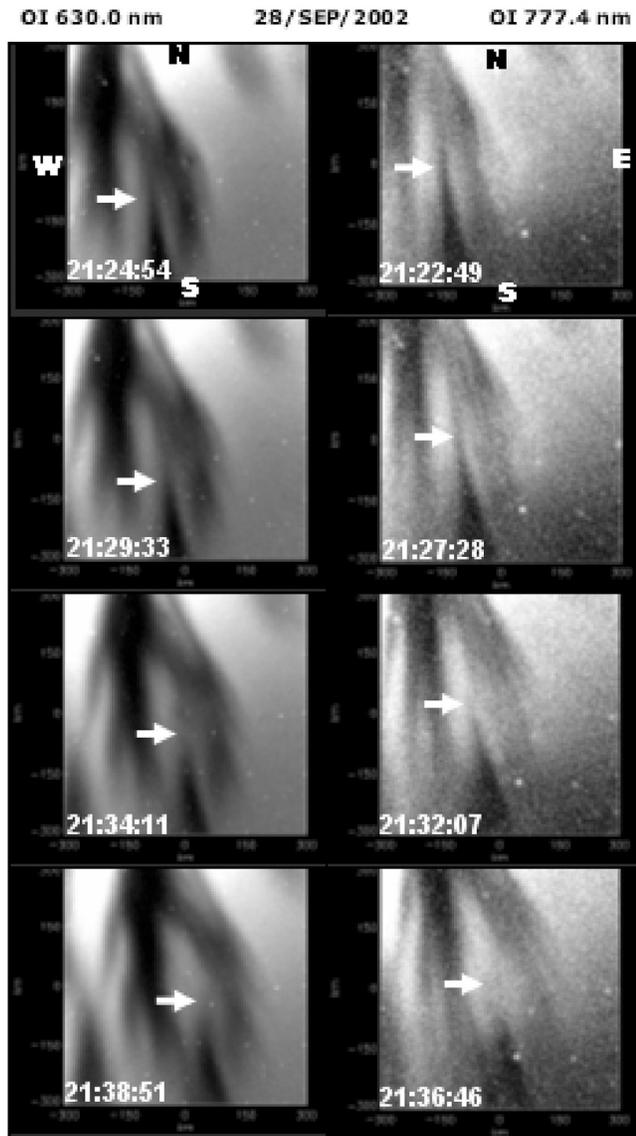


**Figure 2.** Sequence of linearized images (600 x 600 km area) at OI 630.0 nm (assumed peak emission height of 280 km) and OI 777.4 nm (assumed peak emission height of 330 km) emissions on 28 September 2002, showing the evolution (indicated by arrows) of plasma bubble detachment.

more unstable side of an equatorial plasma bubble. Thus, it could be expected that any detached plasma bubble would occur on this side. The observations are continuing and studies of more cases of bubble detachment will be important.

[10] The dynamical structure and time evolution of the observed airglow depletions, presented here, seem to indicate the presence of multiple bifurcating ionospheric plasma bubbles, as they move upward in the low-latitude ionosphere. To properly interpret the dynamics of these depletions seen in the airglow data, the multiple bubble bifurcations in the equatorial upwelling plasma must be mapped to apex height, since the depleted airglow struc-

tures are the optical signatures of plasma depleted flux tubes in the height range where the emissions are generated.

[11] According to the dynamo effect [Rishbeth, 1971], the neutral winds blowing across the magnetic field cause a transverse drift of ions, perpendicular to both the winds and the magnetic field, which sets up an electric polarization field. In the nighttime sector, the generated zonal plasma drifts are eastward and, usually, much stronger than the vertical plasma drifts. During the recent past, wide-angle imaging observations of the F-region nightglow emissions in the equatorial region have been used to study the ionospheric plasma bubble eastward drift velocity [Pimenta *et al.*, 2003b; Martinis *et al.*, 2003; Abalde *et al.*, 2004].

[12] In the computer simulations of ionospheric plasma bubble bifurcations performed by Huang and Kelley [1996], gravity waves are used as seed perturbations to trigger the instability process. The critical quantity determining whether or not a given bubble structure will bifurcate is the ratio of the Pedersen conductivities inside and outside the plasma bubble. They show that the

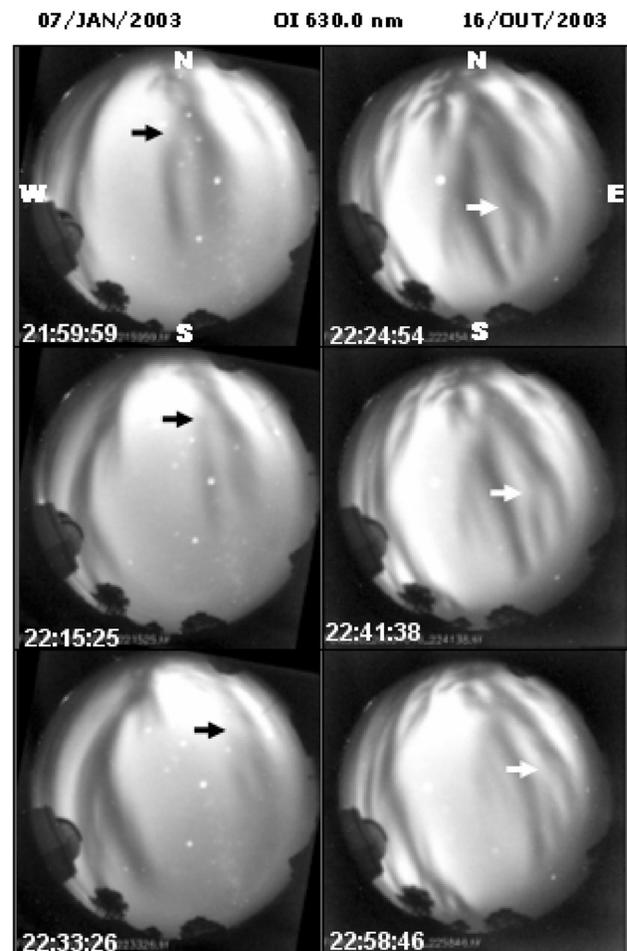


**Figure 3.** Sequence of all-sky images observed at OI 630.0 nm emission on 7 January 2003 and 16 October 2003, showing the evolution (indicated by arrows) of plasma bubble detachment on these two nights.

generated upwelling plasma bubbles begin to bifurcate when they reach the F-peak. In the simulations, *Huang and Kelley* [1996] find that the plasma bubbles bifurcate if their east-west scale size is large (wide bubbles), but they do not bifurcate if their east-west scale size is small (narrow bubbles). The physical explanation for this behavior comes from the argument that the electric field inside a narrow bubble is somewhat homogeneous, so that all charged particles inside the narrow bubble are driven at almost the same velocity by the gravity and the electric field, and the bubble rises upward without bifurcating. On the other hand, for a wide bubble, the internal electric field is inhomogeneous, causing the charged particles to move in different ways inside the upwelling bubble. If the charged particles in the middle of the wide bubble move in opposite directions, toward the bubble walls as it moves upward, they will eventually cause the upwelling bubble to bifurcate [see *Huang and Kelley*, 1996, Figure 3]. This may be caused by an electric field which reverses polarity inside the bubble. Another aspect of the Rayleigh-Taylor instability triggered by gravity waves in the bottomside F-region is the fact that the perturbed plasma density has a steep gradient in the west wall, due to non-linear interaction between gravity waves and plasma drift, which provides a favorable condition for the excitation of smaller scale secondary instabilities. This may result in the generation of multiple plumes on the west wall of the bubble.

[13] *Aggson et al.* [1996] have presented some interesting data on plasma bubble bifurcations, obtained from in situ electric field measurements made from the San Marco D satellite. Their electric field measurements, made across upwelling ionospheric plasma bubbles, indicate that the vertical electric field inside a bifurcating bubble presents a bipolar structure, causing part of the upward moving plasma in the bubble to move westward, and part to move eastward, thus generating the bifurcation of the upwelling bubble.

[14] Their data set also includes extended regions of more variable structures of the vertical electric field in the plasma bubble, with complex and highly variable zonal drift patterns inside the bubble. *Aggson et al.* [1996] also indicate that each branch of the bifurcating bubble structure sometimes exhibit higher frequency electric field wave characteristics, typical of spread F irregularities. The observed zonal plasma flow, associated with plasma density depletions, sometimes is highly irregular, which seems to indicate a more complex or multiple bifurcation process at work. Their data suggest that the occurrence of variable zonal flows inside the upwelling plasma bubble, due to variable polarity vertical electric fields, may be a common feature at higher altitudes in the equatorial ionosphere. The satellite data presented by *Aggson et al.* [1996, Figures 1 and 2] also show the presence of non-homogeneous horizontal electric field inside the bifurcating bubble.

[15] Thus, the bifurcating plasma bubble structure may be the initial step of a cascade sequence of the dynamical evolution of depleted plasma flux tubes into complex and variable smaller scale structures. The observed detached plasma bubble structures, from one of the bifurcated arms, are possibly associated with the development of non-homogeneous vertical plasma drift (the upper part either

moving faster or slower than the lower part) due to non-homogeneous zonal electric field. The possible mechanism for the detachment or tearing off a part of the plasma bubble could be the development of a non-uniform eastward electric field inside the depleted branch (e.g., a stronger or weaker eastward electric field in the upper portion than in the lower portion).

#### 4. Summary

[16] Near-simultaneous all-sky observations, from a low latitude site in the Brazilian sector, of the OI 630.0 nm and OI 777.4 nm emissions on one occasion and all-sky observations of the OI 630.0 nm emission on two occasions show the dynamics of detached equatorial plasma bubbles. These are the first observations reporting the occurrence of detached plasma bubbles. It has been observed that after the bubble bifurcation, the west arm of the bifurcated bubble got detached in all the three cases presented. Obviously, more observations of detached plasma bubbles will be important to investigate this aspect. The observed detached plasma bubble structures are possibly associated with the development of non-homogeneous vertical plasma drift (the upper part either moving faster or slower than the lower part) due to non-homogeneous zonal electric field. Since the observations are continuing on a routine basis, we hope to present more observational results with model calculations in the not too distant future.

[17] **Acknowledgments.** Thanks are due to the Director and staff of “Laboratório Nacional de Astrofísica (LNA)”, for kindly providing all the observational support. Thanks are also due to the Brazilian funding agencies CNPq and FAPESP for the partial financial support through grants 301222/2003-7, 300843/2003-8 and 305625/2003-9 (CNPq) and 2005/00084-3 (FAPESP).

#### References

- Abalde, J. R., P. R. Fagundes, J. A. Bittencourt, and Y. Sahai (2001), Observations of equatorial F region plasma bubbles using simultaneous OI 777.4 nm and OI 630.0 nm imaging: New results, *J. Geophys. Res.*, *106*, 30,331–30,336.
- Abalde, J. R., P. R. Fagundes, Y. Sahai, V. G. Pillat, A. A. Pimenta, and J. A. Bittencourt (2004), Height-resolved ionospheric drifts at low latitudes from simultaneous OI 777.4 nm and OI 630.0 nm imaging observations, *J. Geophys. Res.*, *109*, A11308, doi:10.1029/2004JA010560.
- Aggson, T. L., H. Laakso, N. C. Maynard, and R. F. Pfaff (1996), In situ observations of bifurcation of equatorial ionospheric plasma depletions, *J. Geophys. Res.*, *101*, 5125–5132.
- Dungey, J. W. (1956), Convective diffusion in the equatorial F region, *J. Atmos. Terr. Phys.*, *9*, 304–310.
- Garcia, F. J., M. J. Taylor, and M. C. Kelley (1997), Two-dimensional spectral analysis of mesospheric airglow image data, *Appl. Opt.*, *36*, 7374–7385.
- Huang, C., and M. C. Kelley (1996), Nonlinear evolution of equatorial spread F. 2. Gravity wave seeding of Rayleigh-Taylor instability, *J. Geophys. Res.*, *101*, 293–302.
- Martinis, C., J. V. Eccles, J. Baumgardner, J. Manzano, and M. Mendillo (2003), Latitude dependence of zonal plasma drifts obtained from dual-site airglow observations, *J. Geophys. Res.*, *108*(A3), 1129, doi:10.1029/2002JA009462.
- Mendillo, M., and A. Tyler (1983), Geometry of depleted plasma regions in the equatorial ionosphere, *J. Geophys. Res.*, *88*, 5778–5782.
- Moore, J. G., and E. J. Weber (1981), OI 6300 and 7774 Å airglow measurements of equatorial plasma depletions, *J. Atmos. Terr. Phys.*, *43*, 851–858.
- Ossakow, S. L., S. T. Zalesak, B. E. McDonald, and P. K. Chaturvedi (1979), Nonlinear equatorial spread F: Dependence on altitude of the F peak and bottomside background electron density gradient scale length, *J. Geophys. Res.*, *84*, 17–29.

- Pimenta, A. A., P. R. Fagundes, Y. Sahai, J. A. Bittencourt, and J. R. Abalde (2003a), Equatorial F-region plasma depletion drifts: Latitudinal and seasonal variations, *Ann. Geophys.*, *21*, 2315–2322.
- Pimenta, A. A., J. A. Bittencourt, P. R. Fagundes, Y. Sahai, R. A. Buriti, H. Takahashi, and M. J. Taylor (2003b), Ionospheric plasma bubble zonal drifts over the tropical region: A study using OI 630 nm emission all-sky images, *J. Atmos. Terr. Phys.*, *65*, 1117–1126.
- Rishbeth, H. (1971), Polarization fields produced by winds in the ionospheric F region, *Planet. Space Sci.*, *19*, 357–369.
- Sales, G. S., B. W. Reinisch, J. L. Scali, C. Dozois, T. W. Bullett, E. J. Weber, and P. Ning (1996), Spread *F* and the structure of equatorial ionization depletions in the southern anomaly region, *J. Geophys. Res.*, *101*, 26,819–26,828.
- Weber, E. J., J. Buchau, R. H. Eather, and S. B. Mende (1978), North-south aligned equatorial airglow depletions, *J. Geophys. Res.*, *83*, 712–716.
- Zalesak, S. T., S. L. Ossakow, and P. K. Chaturvedi (1982), Nonlinear equatorial spread F: The effect of neutral winds and background Pedersen conductivity, *J. Geophys. Res.*, *87*, 151–166.
- 
- J. A. Bittencourt, Instituto Nacional de Pesquisas Espaciais (INPE), Cx Postal 515, 12201-970, São José dos Campos, São Paulo, Brazil.
- Y. Sahai, J. R. Abalde, P. R. Fagundes, and V. G. Pillat, Universidade do Vale do Paraíba (UNIVAP), Av. Shishima Hifumi 2911, 12244-000, São José dos Campos, São Paulo, Brazil. (abalde@univap.br)